Supplement of Atmos. Chem. Phys., 19, 14791–14804, 2019
https://doi.org/10.5194/acp-19-14791-2019-supplement

Atmospheric Chemistry and Physics
Open Access
EGU

Supplement of

Effective densities of soot particles and their relationships with the mixing state at an urban site in the Beijing megacity in the winter of 2018

Hang Liu et al.

Correspondence to: Xiaole Pan (panxiaole@mail.iap.ac.cn)

Supplementary

Table. S1 Optical characteristics from the different models

MODEL	DF	DC	DP	CEXT	CABS	CSCA	MEC1064	MAC1064	MSC1064	MAC532	S/C RATIO
C	2	127	194	0.008249	0.007222	0.001028	4.273068	3.740848	0.53225	7.200429	1.527559
C	2.2	127	194	0.008481	0.00731	0.001171	4.392802	3.786476	0.606372	7.288254	1.527559
C	2.4	127	194	0.008713	0.007426	0.001287	4.512995	3.846496	0.666484	7.403781	1.527559
C	2.6	127	194	0.008807	0.007442	0.001365	4.562144	3.85507	0.706998	7.420285	1.527559
C	2.8	127	194	0.008894	0.007465	0.001429	4.607159	3.867013	0.740192	7.443273	1.527559
B	2.6	118	211	0.009052	0.006749	0.002303	5.845469	4.358303	1.487188	8.388915	1.788136
B	2.8	118	211	0.009081	0.006776	0.002306	5.864437	4.37569	1.488904	8.422382	1.788136
C	2	118	211	0.007509	0.00607	0.001438	4.848982	3.920012	0.928948	7.545286	1.788136
C	2.2	118	211	0.007634	0.00607	0.001565	4.930047	3.919786	1.010442	7.544851	1.788136
C	2.4	118	211	0.007902	0.006153	0.00175	5.103241	3.973302	1.129984	7.64786	1.788136
C	2.6	118	211	0.00805	0.006192	0.001859	5.198757	3.998593	1.200255	7.696539	1.788136
C	2.8	118	211	0.008196	0.006236	0.00196	5.292919	4.02727	1.265694	7.751738	1.788136
B	2.4	111	225	0.008644	0.00569	0.002954	6.706476	4.414534	2.292127	8.497148	2.027027
B	2.6	111	225	0.008784	0.005813	0.002971	6.814749	4.509543	2.305237	8.680022	2.027027
B	2.8	111	225	0.008772	0.005799	0.002973	6.805804	4.499055	2.306625	8.659835	2.027027
C	2	111	225	0.006794	0.005059	0.001735	5.270542	3.92499	1.345706	7.554867	2.027027
C	2.2	111	225	0.007256	0.005202	0.002054	5.629294	4.036039	1.593255	7.768617	2.027027
C	2.4	111	225	0.007386	0.005195	0.002191	5.729856	4.030178	1.699492	7.757336	2.027027
C	2.6	111	225	0.007596	0.005246	0.002349	5.892728	4.07028	1.822603	7.834523	2.027027
C	2.8	111	225	0.007747	0.005275	0.002472	6.010565	4.092798	1.917643	7.877867	2.027027
B	2.2	110	238	0.010017	0.005874	0.004144	7.985556	4.682386	3.303418	9.012713	2.163636
B	2.4	110	238	0.010097	0.005946	0.004151	8.049037	4.740193	3.309057	9.123981	2.163636
B	2.6	110	238	0.010119	0.005962	0.004156	8.066415	4.752961	3.313348	9.148556	2.163636
B	2.8	110	238	0.010234	0.006061	0.004174	8.158623	4.831337	3.327179	9.299416	2.163636

C	2	110	238	0.007595	0.005145	0.00245	6.054156	4.101122	1.952927	7.893889	2.163636
C	2.2	110	238	0.007898	0.005171	0.002727	6.296024	4.122401	2.173517	7.934847	2.163636
C	2.4	110	238	0.008168	0.005221	0.002946	6.510939	4.162121	2.348676	8.011301	2.163636
C	2.6	110	238	0.008391	0.00523	0.003161	6.689326	4.169569	2.519899	8.025636	2.163636
C	2.8	110	238	0.0087	0.005315	0.003385	6.93545	4.236597	2.698676	8.154652	2.163636
B	2.2	112	239	0.010308	0.006093	0.004215	7.784914	4.601424	3.183592	8.856876	2.133929
B	2.4	112	239	0.010509	0.006264	0.004245	7.936702	4.730851	3.205648	9.105998	2.133929
B	2.6	112	239	0.010464	0.006224	0.00424	7.902482	4.700357	3.202294	9.047304	2.133929
B	2.8	112	239	0.010527	0.006277	0.00425	7.950255	4.740337	3.210019	9.124258	2.133929
C	2	112	239	0.007729	0.005331	0.002398	5.837076	4.026119	1.811025	7.749522	2.133929
C	2.2	112	239	0.008068	0.005392	0.002676	6.093219	4.072197	2.021225	7.838215	2.133929
C	2.4	112	239	0.008395	0.005429	0.002966	6.340214	4.100319	2.239726	7.892343	2.133929
C	2.6	112	239	0.008832	0.005556	0.003276	6.670218	4.196203	2.47415	8.076902	2.133929
C	2.8	112	239	0.008973	0.005545	0.003428	6.776944	4.187733	2.589144	8.060598	2.133929

Cases 1-5, Models A/B/C from left to right

The fractal prefactor (k_0) is assumed to be 1.2. The monomer size (a) is assumed to be 0.02 μm. The monomer number (Ns) is calculated as the volume-equivalent radii of BC. The wavelength is 1.064 μm.

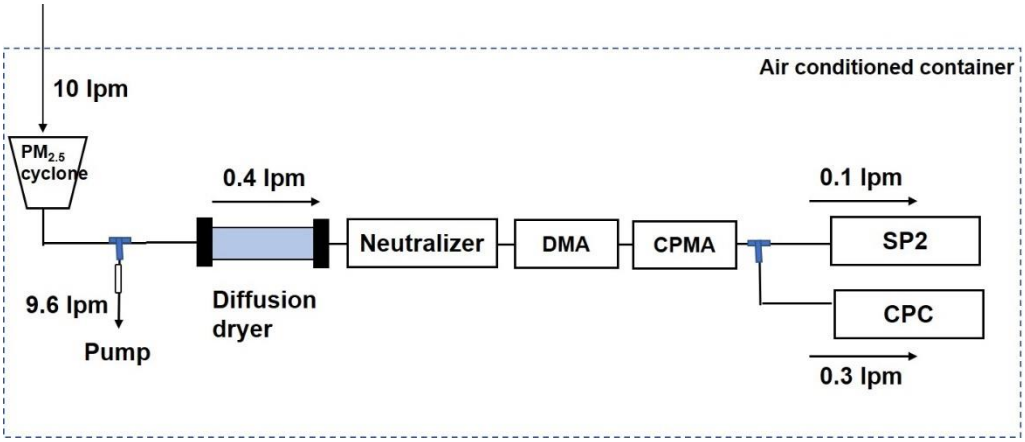

Figure. S1 Schematic diagram of the measurement system.

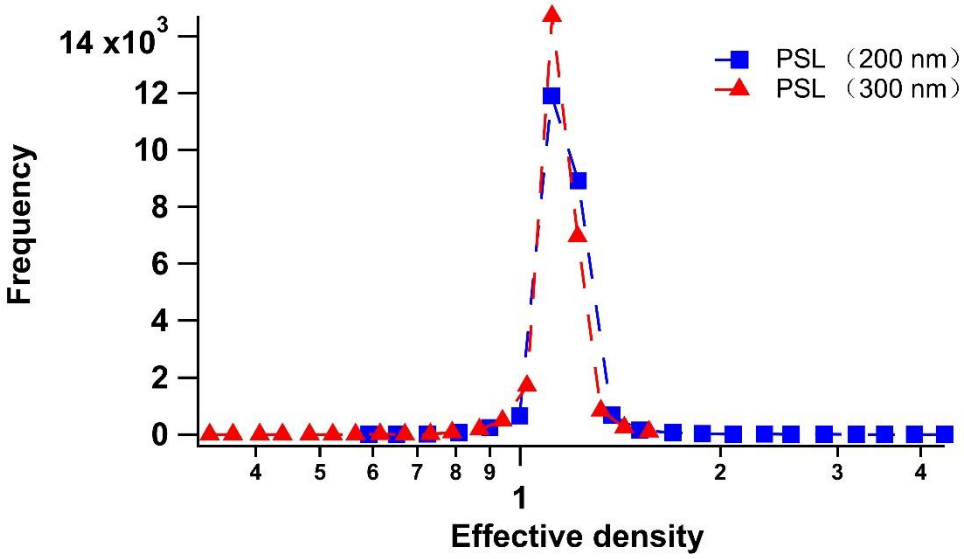

Figure. S2 The effective density distribution of PSL determined by the DMA+CPMA tandem system.

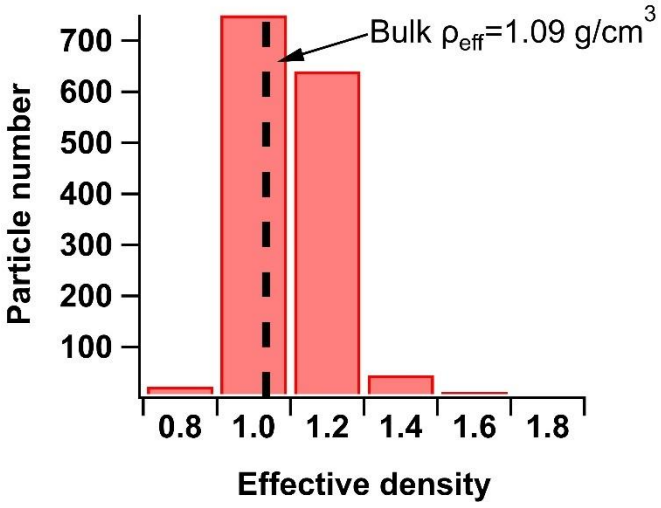

Figure. S3 The weighted average method used to determine the bulk aerosol density of PSL.

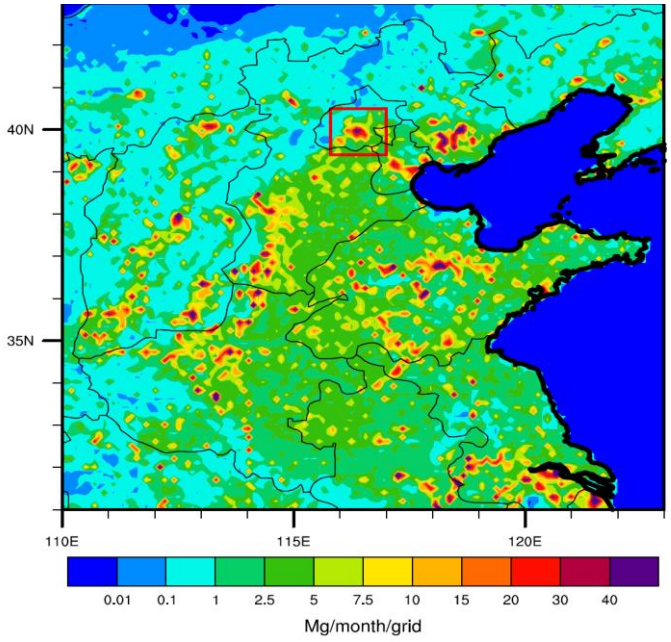

Figure. S4 The emission of rBC in in eastern-central China. The red box denotes the geographical location of the observation site. The map is a built-in map in NCL software (http://www.ncl.ucar.edu/).

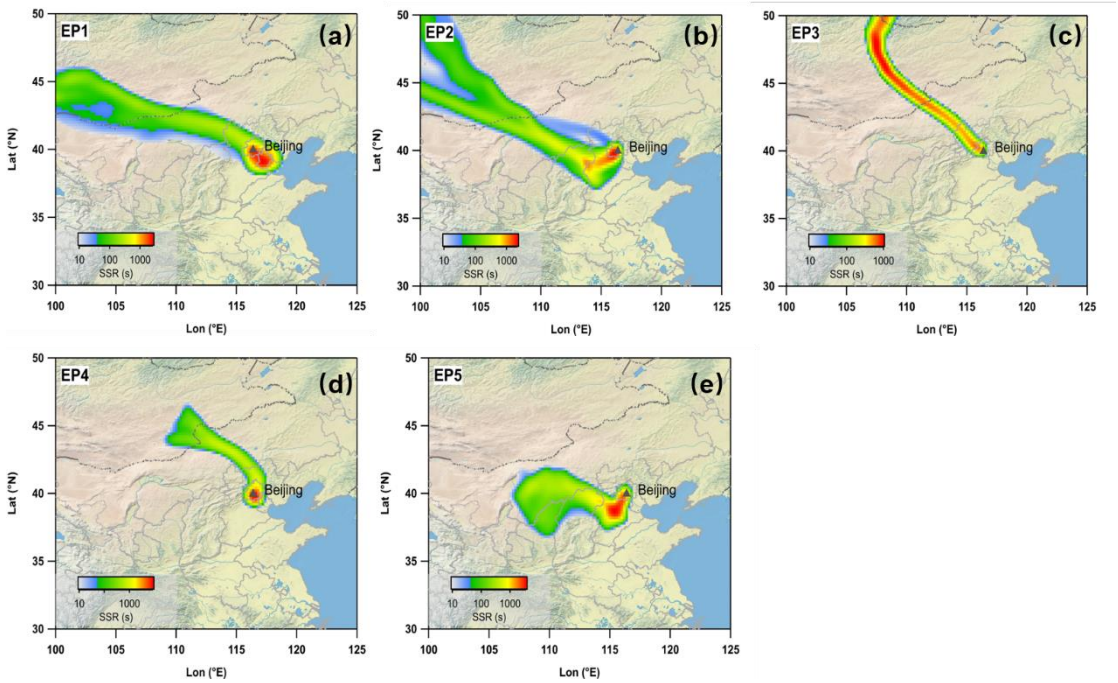

Figure. S5 The 24 h backward trajectories during the five episodes. SSR is the residence time of particles in each cell. The FLEXPART (FLEXible PARTicle) dispersion model (https://www.flexpart.eu, last access: 15 June 2018) developed by the Norwegian Institute for Air Research was used to predicted the backward trajectory. Global Data Assimilation System (GDAS) with 1°×1° resolution was used as the meteorology input

for FLEXPART. Air samples were released at 50m above ground level and the simulation time of backward trajectory is 1 day. The map is a built-in map in IGOR software (https://www.wavemetrics.com/).

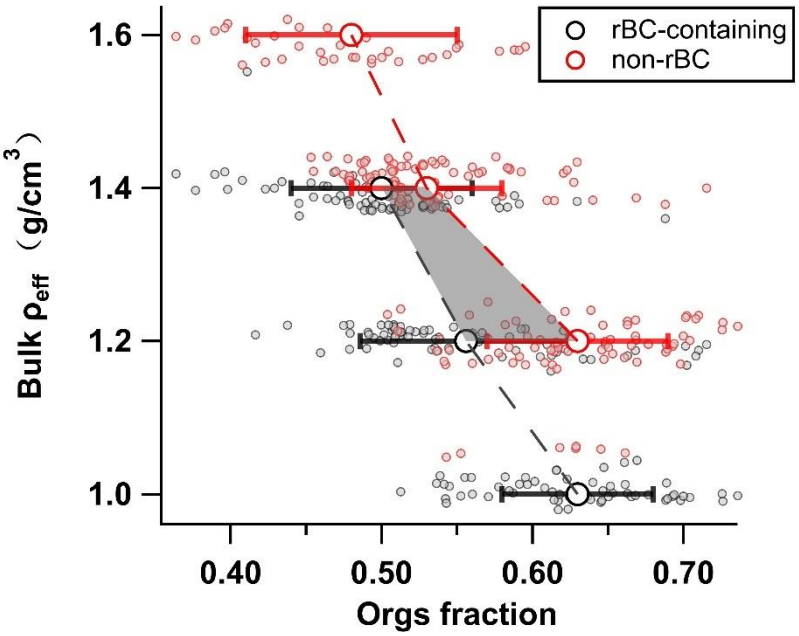

Figure. S6 The relationship between the bulk effective density and the organic mass fraction in the NR-$PM_{2.5}$.

Uncertainty analyze:

The physical parameters directly measured by the tandem system is the mass of rBC-containing particle (M_p), the mass of rBC core (M_{rBC}) and the mobility diameter of rBC-containing particle (D_{mob}).

M_p is selected by CPMA and its uncertainty is influenced by the voltage and rotate speed of CPMA (Olfert and Collings, 2005). In practice, the uncertainty can be determined through setting the resolution (R_m) parameter of CPMA. CPMA can change the voltage and rotate speed automatically to meet the uncertainty which was ~10% during our experiment.

The uncertainty of D_{mob} has been determined to be ~3% (Kinney et al., 1991). The uncertainty of M_{rBC} has determined to be ~30% (Shiraiwa et al., 2008).

For particle density, from the equation

$$\rho_{eff} = \frac{6M_p}{\pi {D_{mob}}^3} \quad (1)$$

Applying the propagation of uncertainty gives:

$$(\frac{\varepsilon_\rho}{\rho})^2 = (\frac{\varepsilon_{M_p}}{M_p})^2 + 9(\frac{\varepsilon_{D_{mob}}}{D_{mob}})^2$$

Then the uncertainty of ρ was determined to be 13.5%.

For dynamic shape factor, from the equation

$$\chi = \frac{D_{mob} \times C_c(D_{mev})}{D_{mev} \times C_c(D_{mob})} \quad (2)$$

Applying the propagation of uncertainty gives:

$$(\frac{\varepsilon_\chi}{\chi})^2 = (\frac{\varepsilon_{D_{mob}}}{D_{mob}})^2 + (\frac{\varepsilon_{Dmev}}{D_{mev}})^2 + 2(\frac{\varepsilon_{C_c}}{C_c})^2 \quad (3)$$

the ε_{Cc}/Cc is the same for all particle sizes and equals to 2.1%(Allen and Raabe, 1985). The D_{mev} is derived from equation 4-5 and the $\varepsilon_{Dmev}/D_{mev}$ is calculated to be ~4% .

$$M_p = \frac{\pi}{6}(D_{mev}^3 - D_c^3) * \rho_{coat} + \frac{\pi}{6} D_c^3 * \rho_{rBC} \quad (4)$$

$$D_{mev} = \sqrt[3]{\frac{6}{\pi}(M_p - \left(1 - \frac{\rho_{coat}}{\rho_{rBC}}\right) * M_{rBC})} \quad (5)$$

Then, the uncertainty of χ was determined to be 5.8%.

For void ratio,

$$R_{void} = 1 - \frac{D_{mev}^3}{D_{mob}^3} \quad (6)$$

$$(\frac{\varepsilon_{\mathrm{Rvoid}}}{R_{void}})^2 = 9\,(\frac{\varepsilon_{D_{mob}}}{D_{mob}})^2 + 9(\frac{\varepsilon_{Dmev}}{D_{mev}})^2 \quad (7)$$

Then, the uncertainty of R_{void} was determined to be 19.6%.

For mass ratio (M_R)

$$M_R = \frac{M_p - M_{rBC}}{M_{rBC}} \quad (8)$$

$$(\frac{\varepsilon_{\mathrm{MR}}}{M_R})^2 = (\frac{\varepsilon_{M_p}}{M_p})^2 + (\frac{\varepsilon_{M_{rBC}}}{M_{rBC}})^2 \quad (9)$$

Then, the uncertainty of M_R was determined to be 31.6%.

Allen, M. D., and Raabe, O. G.: Slip Correction Measurements of Spherical Solid Aerosol-Particles in an Improved Millikan Apparatus, Aerosol Science and Technology, 4, 269-286, Doi 10.1080/02786828508959055, 1985.

Kinney, P. D., Pui, D. Y. H., Mulholland, G. W., and Bryner, N. P.: Use of the Electrostatic Classification Method to Size 0.1 Mu-M Srm Particles - a Feasibility Study, J Res Natl Inst Stan, 96, 147-176, 10.6028/jres.096.006, 1991.

Olfert, J. S., and Collings, N.: New method for particle mass classification - the Couette centrifugal particle mass analyzer, J Aerosol Sci, 36, 1338-1352, 10.1016/j.jaerosci.2005.03.006, 2005.

Shiraiwa, M., Kondo, Y., Moteki, N., Takegawa, N., Sahu, L., Takami, A., Hatakeyama, S., Yonemura, S., and Blake, D.: Radiative impact of mixing state of black carbon aerosol in Asian outflow, Journal of Geophysical Research: Atmospheres, 113, 2008.